

APPLICATION OF NUCLEAR SPECTROSCOPY LOGS TO THE DERIVATION OF FORMATION MATRIX DENSITY

Susan L. Herron and Michael M. Herron
Schlumberger Doll Research
Old Quarry Road
Ridgefield, CT 06877-4108

ABSTRACT

Formation matrix properties, such as matrix density, can be estimated from the elemental concentrations available from modern, openhole, nuclear spectroscopy logging techniques. Although this estimation is similar to that of mineral-based interpretation frequently practiced today, it can preempt the a priori selection of minerals by solving for matrix properties directly from the elements. This simple approach greatly enhances the ability to perform wellsite interpretations in both simple and complex formations.

The interpretation for the matrix density is derived from a comprehensive database containing hundreds of core samples analyzed for both mineralogy and chemistry. The chemical analysis includes not only the major elements, but also the minor and trace elements that significantly influence wireline log responses. These data are used to forward model the matrix which is then solved as a linear combination of four elements (silicon, calcium, iron, sulfur) that are measured by prompt neutron capture spectroscopy. Comparisons are shown between measured and derived matrix density along with statistical measures of goodness of fit. Although in many cases the errors could be reduced by local optimization, the overall agreement is quite good.

Although matrix density is empirically derived, the rationale is straightforward. For example, in sandstone, matrix density is approximately equal to that of quartz and feldspar, and it increases as the concentration of calcium- and iron-bearing minerals increases. Therefore, calcium and iron heavily influence matrix density. The feldspar minerals are less dense than quartz and are not well sensed by the elements Si, Ca, Fe and S. Therefore, separate algorithms are presented for non-arkosic, sub-arkosic, and arkosic environments.

INTRODUCTION

Matrix density, ρ_{ma} , is an important petrophysical parameter needed for the conversion of measured bulk density logs into the desired answer of total porosity. The equation is

$$\phi = \frac{(\rho_{ma} - \rho_b)}{(\rho_{ma} - \rho_f)}, \quad (1)$$

where ρ_{ma} , ρ_b and ρ_f refer to matrix, bulk and fluid densities, respectively. Bulk density is measured by gamma-gamma logging devices. The fluid density can usually be approximated by that of mud filtrate in permeable zones and connate water in less permeable zones – both are close to 1.0 g/cm³. The matrix density is generally unknown in the conversion of bulk density into porosity and for siliciclastic rocks is frequently assumed to be 2.65 g/cm³, the density of quartz.

Matrix density is often estimated as a constant based on local knowledge, or is a byproduct of mineral modeling, which is a common petrophysical analysis procedure today. In mineral modeling, a suite of possible minerals is assumed and log responses are fit as linear combinations of volumes of the possible minerals and fluids such as oil, water and gas. Because there are so few degrees of freedom available from the limited inputs of normal logging suites, the assumed mineral suite may require several processing iterations.

An alternative to mineral modeling is to calculate matrix density from available elemental concentrations.

$$\rho_{ma} = a + b \text{ Si} + c \text{ Ca} + d \text{ Fe} + e \text{ S} \quad (2)$$

The feasibility of this approach has been demonstrated for local optimizations on single well data sets (Herron and Herron, 1997). The goal is to identify a global relationship that does not require local calibration.

JJ

THE DATA SET

The data set consists of 608 siliciclastic samples received from 26 wells around the world which have been analyzed for chemical and mineralogical content. It is important to note that the chemistry and mineralogy are completely independent measurements. Matrix density for each of the samples is computed from the quantitative mineralogy. The reasons for using computed values instead of measured values are presented below.

The quantitative mineralogy was measured using SDR's Dual Range Fourier Transform Infrared (FT-IR) technique (Herron et al., 1997). The mineral concentrations measured are as follows:

Framework Silicates: Quartz, Chert, K-Feldspar, Na-Feldspar, Ca-Feldspar
 Carbonates: Calcite, Dolomite, Ankerite (Fe-rich dolomite), Aragonite, Siderite, Sideroplescite (Mg-rich siderite), Magnesite, High-Mg Calcite
 Clays: Illite, Smectite, Kaolinite, Chlorite, Glauconite
 Others: Muscovite, Biotite, Pyrite, Opal, Gypsum, Anhydrite, Barite, Hematite, Celestite, Fluorite
 Non-FT-IR: Organic matter, salt (halite)

The chemical analyses were performed by X-Ray Assay Laboratories (XRAL) in Don Mills, Ontario, Canada. The analytical techniques include x-ray fluorescence, prompt neutron activation analysis, LECO, coulometry, and induction coupled plasma mass spectrometry. The analysis includes these elements and compounds:

Si, Al, Ca, Mg, Na, K, Fe, Mn, Ti, P, Cr, B,
 Organic C, S, Gd, Th, U, Rb, Sr, Y, Zr, Nb,
 Ba, Cl, H₂O (volatile at low temperature),
 H₂O* (volatile at high temperature), and Loss
 on Ignition (total volatiles).

The matrix density used for this study is calculated from the quantitative mineralogy using the relationship:

$$\frac{1}{\rho_{ma}} = \sum_i \frac{M_i}{\rho_{g_i}} \quad (3)$$

where M_i is the decimal weight fraction of each mineral and ρ_{g_i} is its associated grain density. The assigned grain densities are provided in Table 1 (Hurlbut, 1971; Herron and Matteson, 1993).

There are three major factors that led to the use of computed matrix density for this study. The first is

availability of data. Only a small fraction of the samples analyzed for mineralogy and chemistry were also analyzed for matrix density, and the samples are no longer available. The second factor is sample homogeneity. For the chemistry and mineralogy the samples were scrupulously homogenized and split. In contrast, the matrix densities have generally been measured on separate powdered portions of the sample, and they often show a lack of coherence with the chemistry or mineralogy. The third factor is contamination by organics. The goal of this study is to produce a matrix density of the organic-free matrix. Unfortunately, the core samples obtained for laboratory analysis frequently contain low density (~1.1 g/cm³) insoluble organic matter or a residue of soluble organics following incomplete cleaning, and laboratory measurements of matrix density reflect this organic component. As little as 0.5 wt% organic matter decreases the measured matrix density of a 2.67 g/cm³ sample to 2.65 g/cm³. Therefore, to account for the presence of organics, we have calculated the organic matter for every sample using the organic carbon content, and recomputed the chemistry and mineralogy to provide data on two complete bases: one that includes the organic matter and one that excludes the organic matter from all data. The regressions in this paper are made on an organic-free basis.

The impact of organic matter on measured matrix is demonstrated for three data sets in Figure 1. Figures 1a and 1b show a set of 16 granular samples with an average organic carbon content of 2.6 wt%. Figure 1a shows that the measured matrix density is significantly lower than the matrix density computed on an organic-free mineral matrix. For Figure 1b, the measured organic carbon is treated as an insoluble organic matter and taken into account in the matrix density computation, thus bringing the data sets into fairly good agreement.

A second example is presented in Figures 1c and 1d where measured matrix density values are as low as 2.5 g/cm³. This set of samples contains mostly shales, and the minimum computed matrix density is 2.66 g/cm³. Incorporating the organic matter brings computed matrix densities into reasonable agreement with measured values. Two samples plot off scale due to a large discrepancy, with the measured values at about 3.1 g/cm³ and computed values at 2.65 g/cm³. Neither the chemistry nor the mineralogy of these two samples indicates the presence of a heavy element or heavy mineral, which might explain the high value for the measured density. The discrepancy is therefore

attributed to nonhomogeneity of the samples used for the different measurements.

A final comparison is presented for a set of granular samples containing less than 1 wt% organic carbon in Figures 1e and 1f. For these samples, there is only a small change between the matrix densities computed with and without organic carbon. The agreement between measured and computed matrix densities is fairly good.

THE IMPACT OF MATRIX DENSITY

The impact of matrix density is a function of its variability. Figure 2 presents the matrix density values of the 608 samples in the study data set. Since shales generally have a higher matrix density but are of much less interest from a petrophysics point of view, the samples are sorted on clay content. The clay content is less than 10 wt% in samples up to number 203; less than 20 wt% up to samples 330; and less than 30 wt% up to sample 403. A reference line is drawn for a matrix density of 2.65 g/cm³.

Figure 3 shows the corresponding porosity values assuming a bulk density of 2.4 g/cm³ and a fluid density of 1 g/cm³. The reference line is at 15.15 p.u., corresponding to a fixed matrix density of 2.65 g/cm³.

The most important observation is that for the vast majority of the samples, the matrix density is higher than a commonly used default value of 2.65 g/cm³, and therefore the porosity calculated with the true matrix density is higher. To get a better picture of the increase in porosity, Figure 4 presents the percent change in porosity for samples with less than 20 wt% clay. The very large increases of 40% or greater are unrealistic; they occur primarily in samples with high concentrations of siderite or pyrite that for log data would be accompanied by a compensating increase in bulk density. The real value is in the increases of a few to ten or more percent in porosity; these translate directly into increased estimates of reserves.

The approach here is to compute a level-by-level matrix density as a function of elemental concentrations that can be measured by nuclear spectroscopy. One advantage of this over mineral modeling is that it would enable a wellsite computation. The rationale for estimating matrix density from either minerals or elements is straightforward. Consider a pure quartz sandstone; the matrix density is 2.65 g/cm³. As calcite is substituted for quartz or as the calcium concentration increases, the matrix density increases, approaching

2.71 g/cm³. Similarly, as pyrite or siderite is introduced to the system, the iron concentration increases, and so does the matrix density.

The ability to quantify changes in matrix density from chemistry depends on how well the parameters correlate. The four elements that are readily available for such a computation are silicon, calcium, iron, and sulfur. Figure 5 demonstrates the relationships between these four elemental concentrations and matrix density. There is a high correlation between iron and matrix density. Clearly, in any regression performed on such data, iron will dominate and the other elements will play a moderating role.

The relationship between iron and matrix density can also be observed in some common iron-bearing minerals, as shown in Figure 6. The solid dots represent quartz (no iron), illite, siderite, and pyrite. These are by far the dominant iron-bearing minerals in the data set. For these minerals, the increase in matrix density from quartz to siderite could be modeled on iron alone, and sulfur could be used to provide a boost for the denser pyrite. The open circles represent minerals which are far less common in the study samples but which nevertheless follow the trend of increasing matrix density with increasing iron.

CATEGORIZING THE DATA

Prior to this work, the primary interpretation product for nuclear spectroscopy elemental concentration logs has been SpectroLith* (Herron and Herron, 1996, Horkowitz and Cannon, 1997), a mineral-based lithology determined from elemental concentrations of silicon, calcium, iron, and sulfur. In this interpretation, it was necessary to provide two algorithms for clay determination: a default algorithm, which is fairly robust on a global basis, and a second algorithm for feldspar-rich rocks. In a sandstone classification, the feldspar-rich sandstones in the SpectroLith data set would be classified as sub-arkoses, with a feldspar content ranging from 10-25 wt%. Subsequent research has shown that arkosic sandstones, with feldspar concentrations of greater than 25%, require a different algorithm.

The question arises as to whether similar distinctions must be made for computing matrix density from elements. Since both potassium- and sodium-rich feldspar minerals have a lower matrix density than quartz, it is easy to imagine that extremely high

* Mark of Schlumberger

concentrations of these feldspars would have an impact on the computation. For this study, the individual datasets were categorized as non-arkose, sub-arkose, and arkose. Approximately 68% of the samples fall into the non-arkose category, and these samples are well distributed among varying geographic and geologic regimes. The sub-arkose samples comprise about 19% of the samples, and they also have reasonably diverse origins. Only 13% of the samples are arkoses, and essentially all of these come from multiple wells in the same location. The arkose samples were analyzed, but with such localized sampling, they do not factor heavily in the conclusions. Figure 7 is a histogram of the feldspar content in the samples with less than 20% clay.

ESTIMATION OF MATRIX DENSITY

Regressions to estimate density were performed separately on the following combinations of data:

- | | |
|------------------------------|---------------|
| 1. Non-arkose | (414 samples) |
| 2. Non-arkose and sub-arkose | (530 samples) |
| 3. Sub-arkose | (116 samples) |
| 4. Arkose | (76 samples) |

The data were analyzed using a least squares regression to predict matrix density (in g/cm³) from silicon, calcium, iron, and sulfur (expressed in wt%) on each of the data sets described above. Since the primary objective is to develop an interpretation for nuclear spectroscopy logging devices, the known elemental interferences for calcium and iron were taken into account, so the regressions were actually run using the quantities Ca+0.6Na and Fe+0.14Al (Herron et al., 1992).

Table 2 presents the results of the regressions, including the intercepts and elemental coefficients as well as the correlation coefficient and standard error. For all categories analyzed, the standard error of the estimated matrix density is better than 0.016 g/cm³. The algorithms for non-arkose (Algorithm 1) and the combined non-arkose/subarkose (Algorithm 2) are essentially identical. Algorithm 2 is demonstrated on data from six wells in Figure 8. The wells in the left and center columns are non-arkosic; the wells in the right column are sub-arkosic. The standard error ranges from 0.005 g/cm³ for one of the subarkose datasets to 0.026 g/cm³ for one of the non-arkose datasets. These are the best and worst levels of agreement. The subarkose algorithm (3) produces a matrix density approximately 0.01 g/cm³ less than algorithm 2. However, it only provides a substantive improvement to

matrix density estimation in one of nine subarkose datasets. Overall, the combined non-arkose/subarkose algorithm is quite robust and serves both categories well as a default estimator of density.

In contrast, the arkose algorithm (4) produces matrix densities that are as much as 0.06 g/cm³ lower than algorithm 2. The difference is greatest in the sands and approaches zero in the shales. These rocks have greater than 40 wt% feldspar, and must be interpreted differently. It is important to note that this algorithm is derived using samples from a single geographical location, and it is not necessarily representative of all arkosic rocks.

Figure 9 presents an example of matrix density derived by applying algorithm 2 to elemental concentration logs from a deltaic depositional environment in Venezuela (Bryant et al., 1997). A 2.65 g/cm³ reference line is provided. Core data are shown for comparison. The core matrix density ranges from 2.66 to 2.76 g/cm³, and the variations are predicted quite well by the log data.

CONCLUSIONS

A robust estimation of matrix density from log-derived elemental concentrations has been presented. This estimation was derived using a core database of over 600 sands and shaly sands. The matrix density estimation provided is free of organics; it represents the mineral matrix. A single algorithm can be used for non-arkosic and subarkosic environments with standard errors of about 0.015 g/cm³. The input elemental concentration logs are available at the wellsite. Thus, a real time matrix density is easily feasible from the current generation of nuclear spectroscopy logs.

ACKNOWLEDGMENTS

We thank A. Matteson, Manager of Petrophysical Laboratories at SDR, M. Polyakov, W. Smith, and M. Schwartz for core measurements. J. Grau processed the nuclear spectroscopy log data.

REFERENCES

Bryant, I.D., Herron, M. M. and Gamero de Villarroel, H., 1997, Application of sequence stratigraphic reinterpretation of Lower Lagunillas Member to further development of Bloque IV, Lake Maracaibo, Venezuela, SPE Formation Evaluation, Vol 12, No 4, pp. 271-279.

- Herron, M. M., Dove, R. E. and Grau, J. A., 1992, Compensation for mineral sodium interference in Ca and Gd thermal neutron capture gamma-ray logging measurements, Nuclear Geophysics, Vol. 6, No. 2, pp. 173-180.
- Herron, M. M. and Herron, S. L., 1997, Log interpretation parameters determined from chemistry, mineralogy and nuclear forward modeling, Proceedings of the 1997 International Symposium of the Society of Core Analysts, Calgary, 7-10 September, SCA-9727, 12 p.
- Herron, M. M. and Matteson, A., 1993, Elemental composition and nuclear parameters of some common sedimentary minerals, Nuclear Geophysics, Vol. 7, No. 3, pp. 383-406.
- Herron, M. M., Matteson, A. and Gustavson, G., 1997, Dual-range FT-IR and the analysis of sedimentary formations, Proceedings of the 1997 International Symposium of the Society of Core Analysts, Calgary, 7-10 September, SCA-9729, 12p.
- Herron, S. L. and Herron, M. M., 1996, Quantitative Lithology: An application for open and cased hole spectroscopy, Transactions of the SPWLA 37th Annual Logging Symposium, New Orleans, LA, June 16-19, Paper E.
- Horkowitz, J. P. and Cannon, D. E., 1997, Complex reservoir evaluation in open and cased wells, Transactions of the SPWLA 38th Annual Logging Symposium, Dallas, TX, June 15-18, Paper W.
- Hurlbut, C. S., 1971, Dana's Manual of Mineralogy, John Wiley and Sons, New York, 579 p.

ABOUT THE AUTHORS

Susan Herron is Program Manager of Formation Evaluation Nuclear in the Reservoir Definition/Evaluation Research Group at Schlumberger-Doll Research. She joined Schlumberger in 1984 and has worked on applications of nuclear spectroscopy logs. Susan holds a PhD in Geological Sciences from the State University of New York at Buffalo.

Michael Herron is a Scientific Advisor in the Reservoir Definition Evaluation Research Group at Schlumberger Doll Research. He joined Schlumberger in 1982. He holds a B.A. in chemistry from University of California at San Diego and a PhD in Geological Sciences from the State University of New York at Buffalo.

Table 1. Mineral Grain Densities

Mineral	Grain Density	Mineral	Grain Density
Quartz	2.65	Pyrite	5.01
Opal	2.1	Hematite	5.26
Chert	2.65	Siderite	3.9
Orthoclase	2.55	Sideroplescite	3.71
Albite	2.62	Calcite	2.71
Anorthite	2.76	Dolomite	2.85
Illite	2.8	Ankerite	2.97
Smectite	2.78	Aragonite	2.95
Kaolinite	2.63	High-Mg Calcite	2.7
Chlorite	3.07	Magnesite	3.1
Glauconite	2.89	Fluorite	3.18
Muscovite	2.8	Celestite	3.95
Biotite	3.0		

Table 2. Matrix density coefficients

	No. of Samples	Algorithm	Intercept	Si	Ca+0.6Na	Fe+0.14Al	S	r	Std error
Non-arkose	414	1	2.625	0.0439	0.2277	1.992	1.144	0.971	0.016
Non-arkose & subarkose	530	2	2.620	0.0490	0.2274	1.993	1.193	0.967	0.015
Subarkose	116	3	2.750	-0.2472	-0.1467	1.020	1.020	0.933	0.008
Arkose	76	4	2.851	-0.5741	-0.3572	0.9950	1.341	0.984	0.004

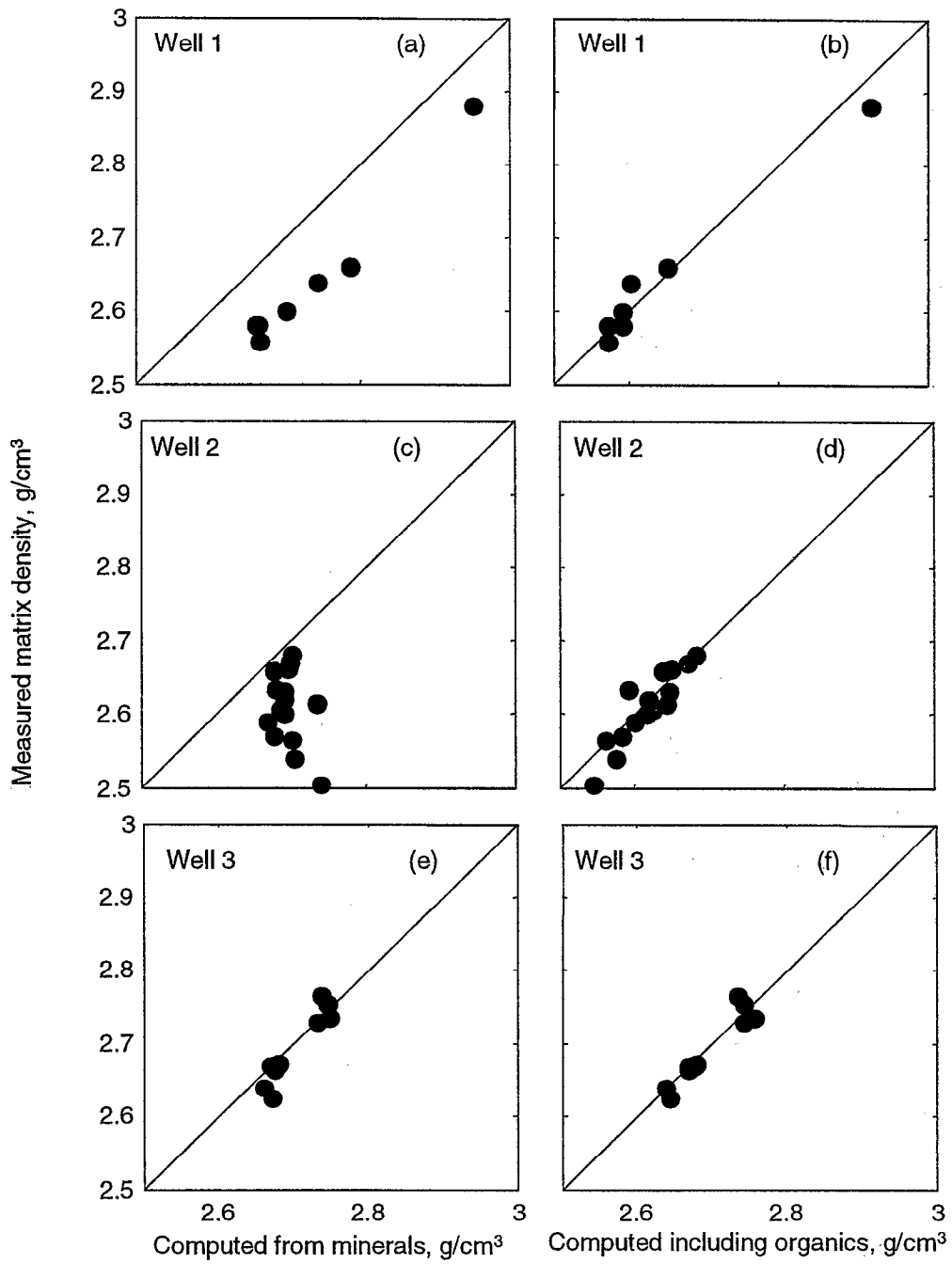


Figure 1. The presence of organic matter in samples from wells 1 and 2 lowers the measured matrix density as compared to the matrix density computed from minerals, as seen in Figures 1a and 1c. When organic matter is incorporated into the computation, the two values agree much more closely. In well 3, the organic content is less than 1 wt%, so the impact is considerably smaller.

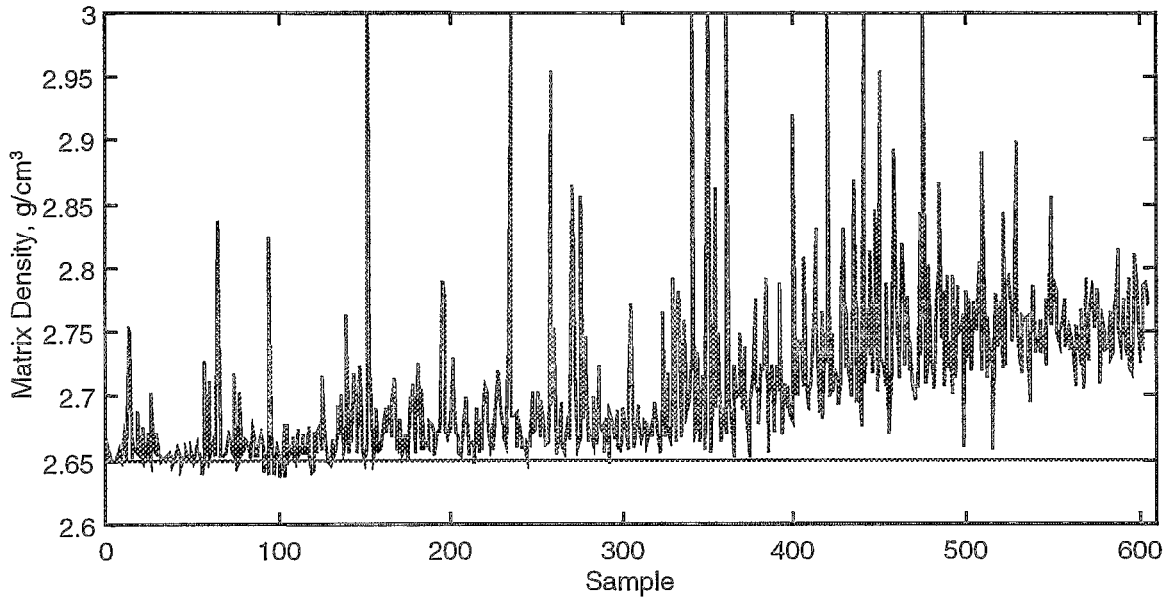


Figure 2. Matrix densities on all samples ordered by increasing clay content. Note the generally higher matrix densities in the shalier samples.

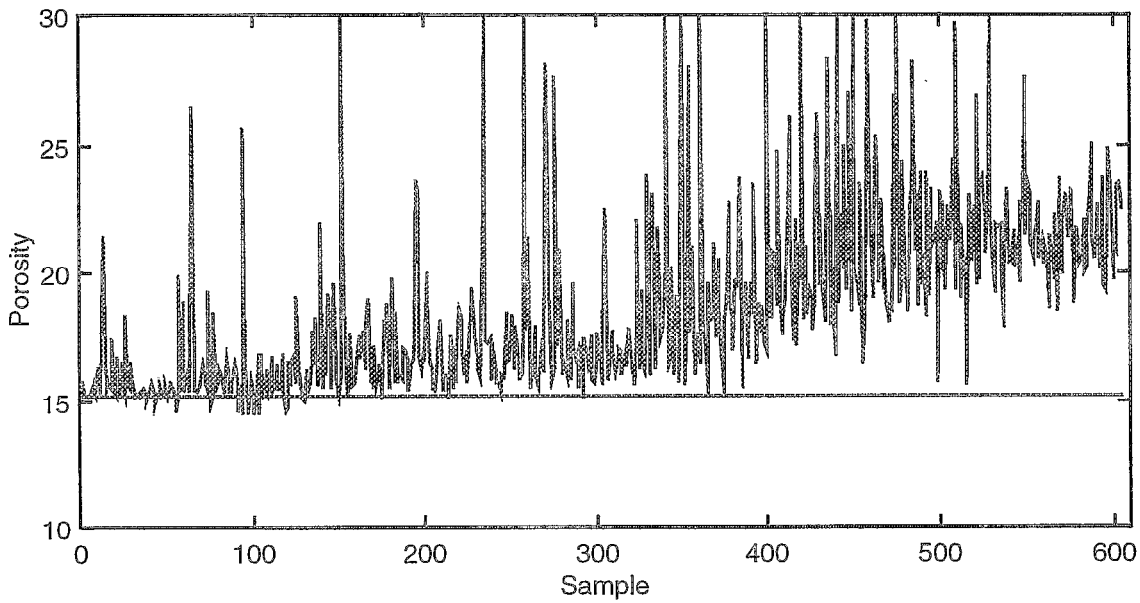


Figure 3. The matrix densities from Figure 2 are translated into porosity values assuming a bulk density of 2.4 g/cm^3 and a fluid density of 1.0 g/cm^3 . The straight, horizontal line represents a porosity of 15.15 p.u., the value calculated from a matrix density of 2.65 g/cm^3 .

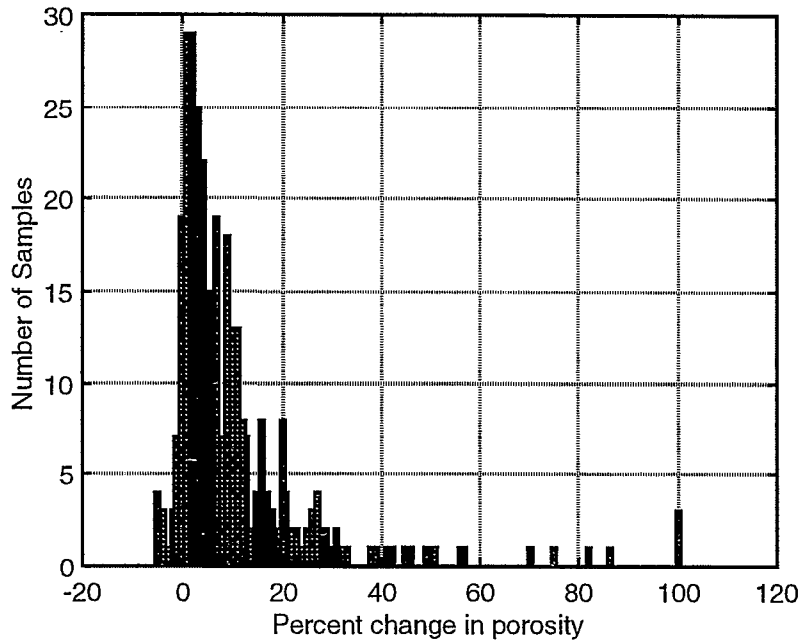


Figure 4. Percentage change in porosity using measured matrix density instead of a default 2.65 g/cm³.

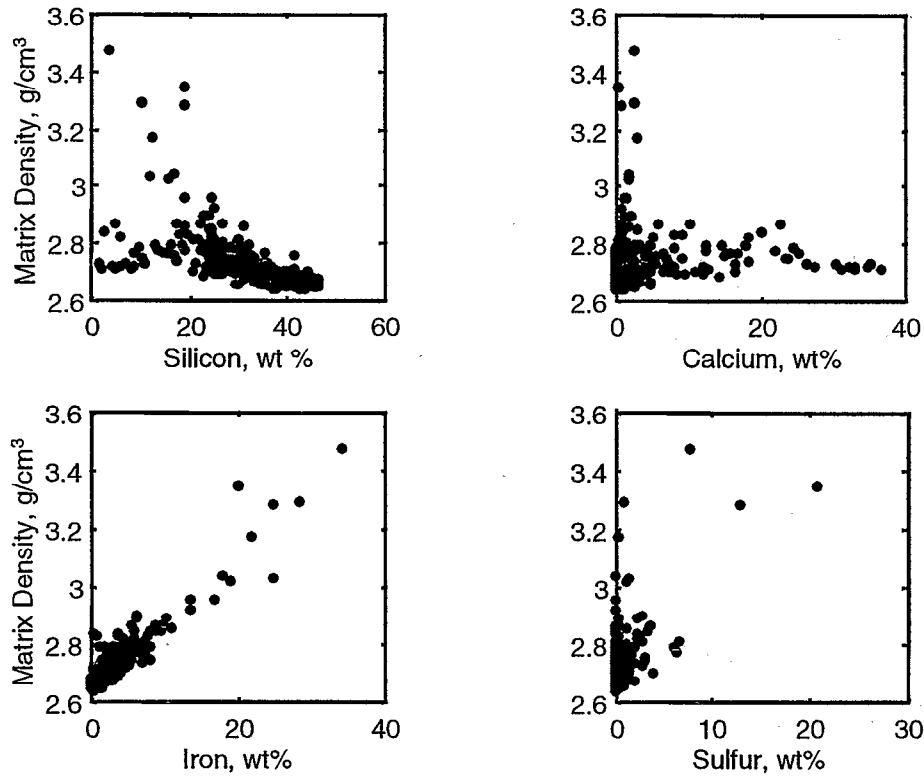


Figure 5. Matrix densities compared to concentrations of silicon, calcium, iron, and sulfur. Note the strong correlation between matrix density and iron.

JJ

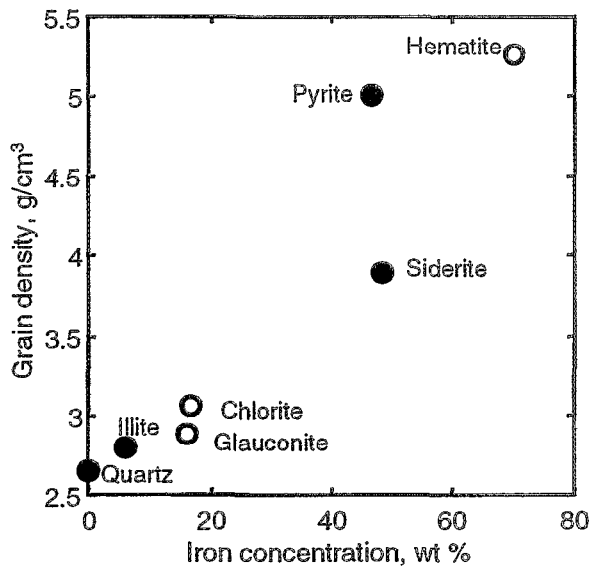


Figure 6. Relationship between grain density and iron concentration in quartz and some iron-bearing minerals (Hurlbut, 1971; Herron and Matteson, 1993). Solid dots represent the more common minerals.

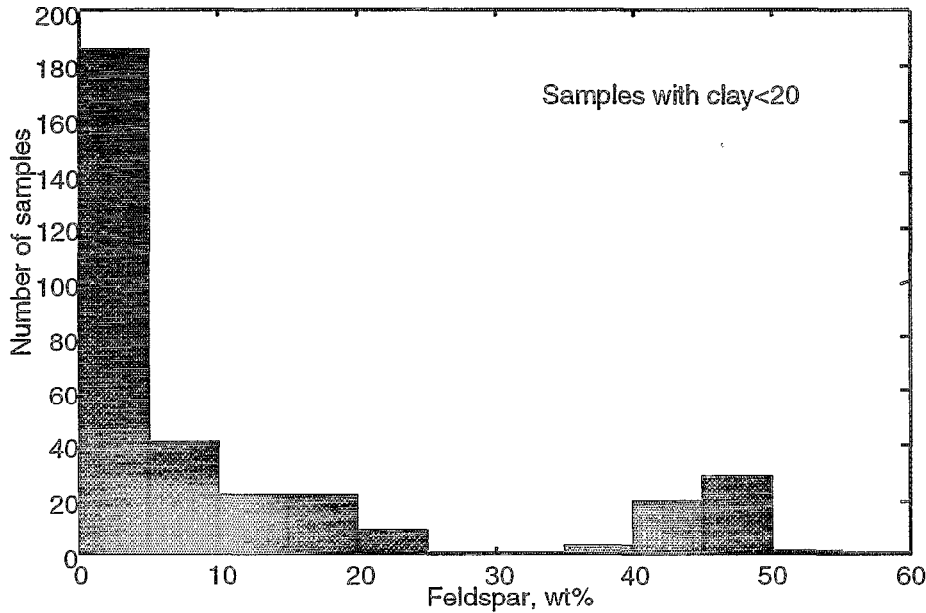


Figure 7. Feldspar content of sandstone samples with total clay concentrations of less than 20 wt%. The majority of samples in this study belong to the non-arkosic category (<10 wt% feldspar).

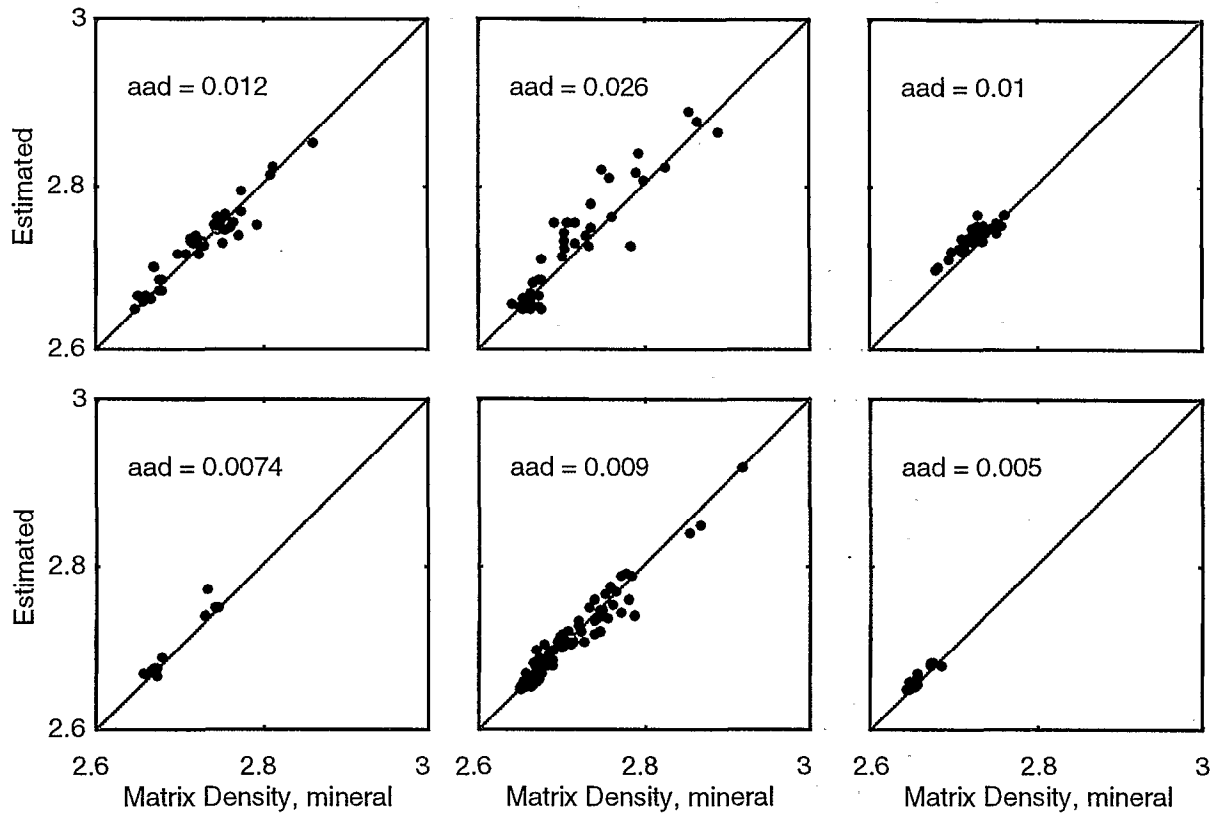


Figure 8. Comparison of measured and estimated matrix densities from algorithm 2 for six wells. Wells in the first two columns are non-arkosic; wells in the third column are subarkosic. The average absolute deviation between measured and estimated matrix density is provided for each well. These six wells span the range from the best to worst agreement.

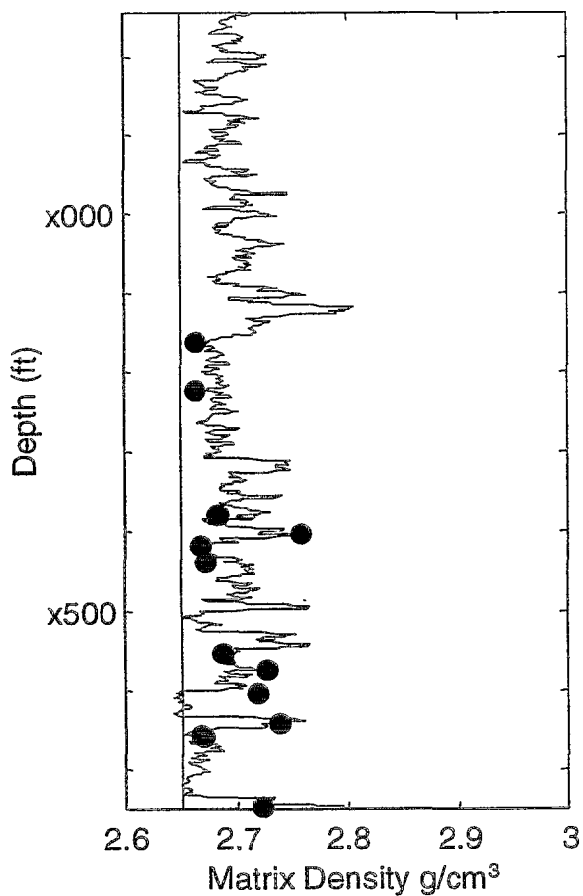


Figure 9. Matrix density log for a well in Venezuela (Bryant et al., 1997) computed from nuclear spectroscopy log data. Core matrix densities are in good agreement with the log values. The vertical line represents a matrix density of 2.65 g/cm³.